Available online at www.sciencedirect.com
ScienceDirect
Trans. Nonferrous Met. Soc. China 32(2022) 569−580
Transactions of Nonferrous Metals Society of China
www.tnmsc.cn

Biocompatibility of vascular stents manufactured using metal injection molding in animal experiments

Chang SHU[1,2*], Hao HE[1*], Bo-wen FAN[2], Jie-hua LI[1], Tun WANG[1], Dong-yang LI[3], Yi-min LI[3,4], Hao HE[4]

1. Department of Vascular Surgery, Second Xiangya Hospital, Central South University, Changsha 410011, China;
2. Department of Vascular Surgery, Fuwai Hospital,
Chinese Academy of Medical Science, Beijing 100037, China;
3. State Key Laboratory of Powder Metallurgy, Central South University, Changsha 410083, China;
4. School of Microelectronic and Materials Engineering, Guangxi University of Science and Technology,
Liuzhou 545006, China

Received 6 March 2021; accepted 17 August 2021

Abstract: This study aimed to evaluate the feasibility and safety of a novel stent manufactured by metal injection molding (MIM) in clinical practice through animal experiments. Vessel stents were prepared using powder injection molding technology to considerably improve material utilization. The influence of MIM carbon impurity variation on the mechanical properties and corrosion resistance of 316L stainless steel was studied. In vitro cytotoxicity and animal transplantation tests were also carried out to evaluate the safety of MIM stents. The results showed that the performance of 316L stainless steel was very sensitive to the carbon content. Carbon fluctuations should be precisely controlled during MIM. All MIM stents were successfully implanted into the aortas of the dogs, and the MIM 316L stents had no significant cytotoxicity. The novel intravascular stent manufactured using MIM can maintain a stable form and structure with fast endothelialization of the luminal surface of the stent and ensure long-term patency in an animal model. The novel intravascular stent manufactured using MIM demonstrates favorable structural, physical, and chemical stability, as well as biocompatibility, offering promising application in clinical practice.
Key words: vascular stent; metal injection molding; cytotoxicity test; animal experiment; biocompatibility

1 Introduction

Vascular stents are widely used to treat coronary and peripheral artery disease owing to their excellent therapeutic effect, high rate of technical success, and very low mortality and morbidity [1−3]. In the field of stents preparation, braiding or laser cutting techniques have been widely recognized and these stents occupy most of the market share; however, they also have certain disadvantages such as the high cost of equipment, high production cost, and poor geometric properties, such as more nodes on the surface and a greater metal surface area, which can significantly increase the risk of thrombosis and restenosis rate after stent implantation [4−6].

Thus, researchers have explored other technologies to prepare stents, including near-net-shape technology, which has shown promising potential; meanwhile, biodegradable stent materials have also been investigated [7,8]. At present, studies on 3D printed blood vessel stents have been reported [9−11]; however, only polymer materials with simple shapes and rough surfaces have been investigated.

Corresponding author: Chang SHU, Tel: +86-10-88322371, E-mail: shuchang@csu.edu.cn;
Yi-min LI, +86-731-88830693, E-mail: 100001866@gxust.edu.cn
Chang SHU and Hao HE contributed equally to this work
DOI: 10.1016/S1003-6326(22)65816-3

Metal injection molding (MIM) has been rapidly developing owing to its ability to manufacture complex shapes at a low production cost per part (in bulk volume production). MIM has been applied to the production of various medical products, such as scalpels, buccal tubes, and bone implants [12]. Additionally, the related alloys manufactured using MIM have also shown good biocompatibility [13]. However, the potential of using MIM for manufacturing novel stents has not been sufficiently recognized. There are very few studies related to this field. In US patent US8303642 B1, the MIM technique was first used to produce thin-wall stainless steel tubes; secondary machining or laser cutting was needed to generate pores on the tubes [14]. MARIOT et al [15] produced pure iron dog-bone-shaped parts using MIM and investigated their in vitro degradation rates. However, there have been no reports on the biomedical application and commercial-scale manufacturing of vascular stents using the MIM method.

This study attempted to use MIM as a direct preparation technology for scaffolds. Stents were implanted into the iliac arteries of adult dogs using a standard angioplasty technique. The MIM processing parameters, stent properties, status of experimental animals, and endothelialization of implanted stents were investigated, and a molecular biology evaluation was carried out.

2 Experimental

2.1 Materials preparation and characterization

The raw material used in this study was gas-atomized 316L stainless steel powder (D_{50}=12.5 μm) provided by Hunan Hengji Powder Technology Co., Ltd., China. The morphology of the powders is shown in Fig. 1(a). The powder was mixed with a multicomponent binder system consisting of paraffin wax and low-density polyethylene (LDPE). The powder and binder were mixed using a blade mixer at 160 °C for 3 h, using a powder loading of 60%−65%. Standard tensile specimens and stents were molded using a BOY 50T2 injection molding machine. After solvent debinding and thermal debinding, the 316L specimens were sintered at 1340 °C and 0.1 Pa. Debinding residue is a problem that must be overcome in the MIM process. To study the effect of carbon content fluctuation on the mechanical and corrosion properties of 316L stainless steel, 0−0.4 wt.% graphite was added, following which performance evaluation was carried out. The topography of the graphite is shown in Fig. 1(b). The nominal and sintered carbon contents are listed in Table 1.

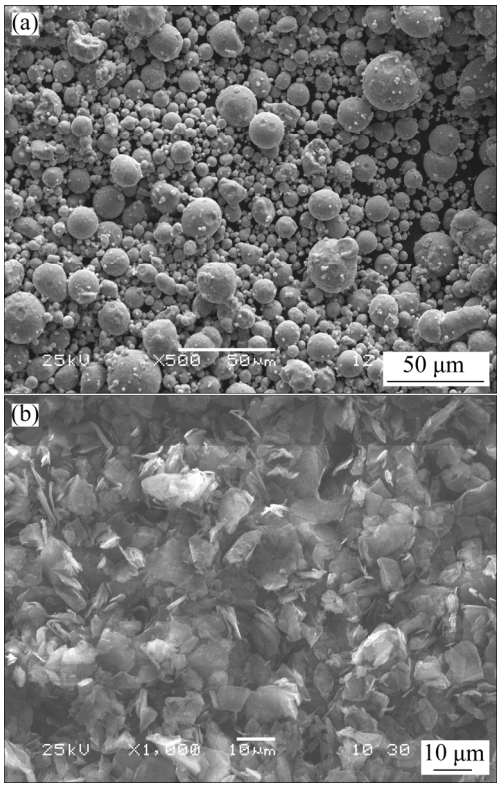

Fig. 1 SEM images of 316L stainless steel (a) and graphite (b)

Table 1 Nominal and sintered contents in MIM 316L stainless steel

No.	Carbon addition/wt.%	Sintered carbon content/wt.%
1	0	0.10
2	0.1	0.15
3	0.2	0.18
4	0.3	0.30
5	0.4	0.35

The density of the sintered samples was measured using the Archimedes method. The tensile properties of the samples were measured using an Instron materials testing system. Hardness was tested using the 1875 Brinell hardness tester. The metallograph was studied using a JSM−6360 scanning election microscope. Oxygen and carbon

analyses were carried out using LECO TCH−600 and LECO CS−600 analyzers, respectively.

2.2 In vitro cytotoxicity experiments

Liquid extracts of the MIM stent, polyethylene, as a negative control, and polyurethane (Sigma-Aldrich), as a positive control, were obtained according to ISO 10993 — 12. The materials were immersed in an endothelial cell culture medium (ECM), with 5% fetal bovine serum (FBS), 1% endothelial cell growth supplement, and 1% penicillin/streptomycin solution (ScienCell) at 37 °C for 24 h. Human umbilical vein endothelial cells (HUVECs) (104 cells/well) were planted in a 96-cell plate. Cell viability was assessed using the cell counting Kit 8 (CCK-8, Dojindo Molecular Technologies) at 24, 48, and 72 h, according to the manufacturer's instructions.

2.3 In vivo animal study

Because the canine vascular response is relevant to humans, similar studies have been conducted for stent histology [16]. Eight healthy, adult dogs (average mass: (14.24 ± 0.88) kg, average age: (1552 ±177.3) d) were studied. All experimental procedures were approved by the Institutional Animal Care and Use Committee of Central South university, China, and the dogs were housed under the supervision of a licensed veterinarian within the regulations of the Ministry of Health, China. With oxygen supplied at 2 L/min through a face mask, xylazine sedation (9.3 mg/kg) (Bayer HealthCare, Kiel, Germany) and tiletamine-zolazepam anesthesia (10 mg/kg) (Virbac, Carros, France) were administered by intramuscular injection. The novel stent was fixed and assembled manually between the markers of a suitable balloon dilation catheter, ensuring no forward or backward movement relative to the balloon and the stent. The MIM stent, fixed on the balloon catheter, could therefore advance through the guidewire to the target iliac artery from the exposed carotid artery. The balloon was dilated at 8.104×10^5 Pa for 15 s to release the stent into the iliac artery; then, the balloon and guidewire were retrieved, and angiography was performed to check the results of the procedure.

The dogs were randomly separated into two groups, which were observed for 1 and 6 months after the operation, respectively. During the observation period, the physical and mental status of the dogs was recorded. Aspirin (150 mg) and dipyridamole (25 mg) were administered daily for 1 month and then discontinued. Digital subtraction angiography (DSA) was performed on all the dogs before sacrifice to evaluate the shape, location, and patency of the novel stent in the iliac arteries of the dogs. Sacrifice was performed in accordance with the Care and Use of Laboratory Animals outlined by the Ministry of Science and Technology of China.

During the autopsy of each dog, the stented iliac artery was observed to see if there were any adverse events, including in-stent thrombosis, in-stent stenosis, and stent infection. In addition, the stent surface was observed to determine the extent of the endothelization procedure. For each dog, the vascular wall of the stented common iliac artery was collected for samples, and the vascular wall of the contralateral common iliac artery was used as the control sample. Geometrical parameters were measured and recorded for each sample. Then, the samples were numbered and preserved under different conditions for morphological observation under a light microscope (TUNEL) and a scanning electron microscope. Molecular biology evaluation was performed using quantitative real-time polymerase chain reaction (qPCR) to determine the expression levels of CD31, CD34, CD133, and endothelial nitric oxide synthase (eNOS).

2.4 Statistical analysis

SPSS (Version 20.0; Chicago, IL, USA) for Windows was used for statistical analysis. The data were expressed as (mean ± standard deviation) (SD, %). Student's *t*-test was used for continuous data, and Pearson's Chi-square or Fisher's exact test was used to compare categorical data. All tests were two-sided, and P values less than 0.05 were considered to be statistically significant.

3 Results and discussion

3.1 Effect of carbon content on MIM 316L stainless steel

Carbon content fluctuation is a common problem encountered in the MIM process, mainly due to binder residue and poor processing control. Carbon has a high affinity to combine with Cr and

other elements in stainless steel to form carbides. The presence of carbides can promote the liquid phase and enhance the densification process. In contrast, if these carbides form a continuous phase along the grain boundary, the ductility of the sintered samples will be degraded.

Figure 2(a) shows the tensile strength, elongation, and hardness of MIM 316L stainless steel with different carbon contents. As the carbon content increased, the tensile strength increased from 480 to 585 MPa at a carbon content of from 0.1 wt.% to 0.30 wt.% and then decreased to 460 MPa at a carbon content of 0.35 wt.%. The hardness of the sintered sample increased with increasing carbon content, while the elongation decreased, particularly when the carbon exceeded 0.30 wt.%. The corresponding microstructures and tensile fracture morphologies are shown in Figs. 3(a–d) and (e–h), respectively. As the carbon content increased, the number of pores decreased. The size of the pores was small when the carbon content was below 0.18 wt.%, while large pores could be clearly observed in samples with a carbon content greater than 0.3 wt.%. Grain growth was evident when the carbon content exceeded 0.3 wt.%, which accounted for the drastic drop in tensile strength and elongation. At the same time, at a high carbon content, the fracture surface showed more obvious brittle fractures.

Figure 2(b) shows the corrosion rates of the MIM 316L stainless steel in different solutions. The corrosion resistance decreased with increasing carbon content, particularly in the NaCl solution. A considerably faster corrosion rate was observed when the carbon content exceeded 0.3 wt.%. Nevertheless, the corrosion resistance of the MIM 316L stainless steel stents with a carbon content below 0.2 wt.% is acceptable. Carbon combines with Cr to form carbide, which degrades the Cr content in the matrix and hence accelerates corrosion. In HCl solution, the corrosion rate is considerably higher than that in NaCl solution when

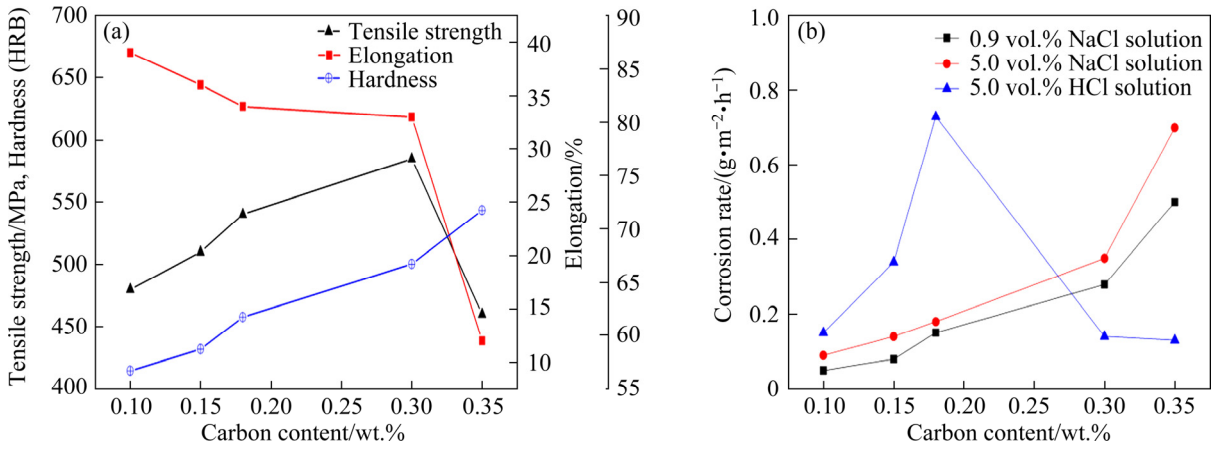

Fig. 2 Mechanical properties (a) and corrosion rate (b) of MIM 316L stainless steel with different carbon contents

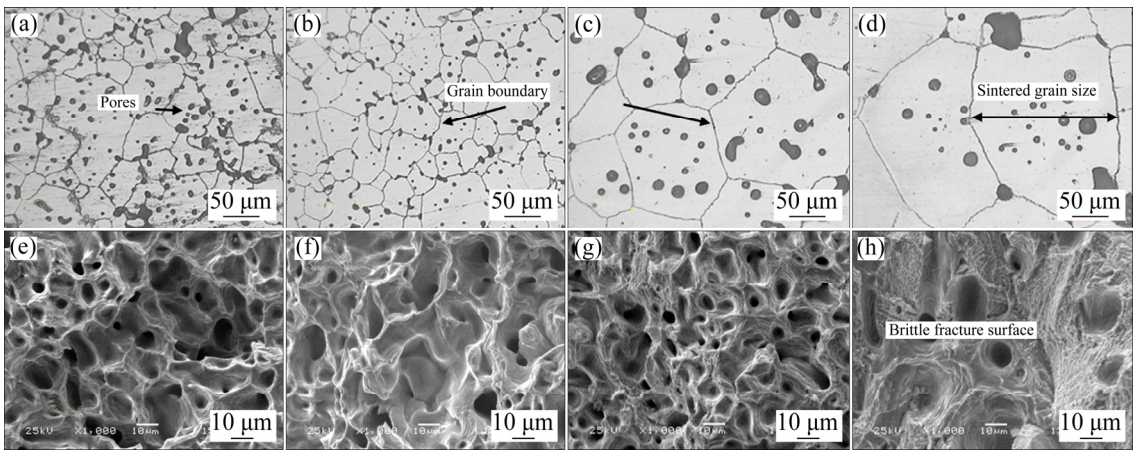

Fig. 3 Microstructures after etching (a–d) and tensile fracture morphologies (e–h) of 316L stainless steel with different carbon contents: (a, e) 0.10 wt.%; (b, f) 0.18 wt.%; (c, g) 0.30 wt.%; (d, h) 0.35 wt.%

the carbon content is not greater than 0.2 wt.%. However, beyond this, the corrosion rate in HCl solution is lower than that in NaCl solution. Further investigations are required to elucidate this mechanism.

The mechanical properties and corrosion resistance of 316L stainless steel are extremely sensitive to the fluctuation in the carbon content. The carbon content needs to be precisely controlled according to the performance requirements of MIM vascular stents.

The 316L stainless steel stents prepared using MIM technology must be mechanically reliable. If the MIM process is stable and the carbon impurities are properly controlled, the mechanical properties of MIM 316L stainless steel can be comparable to those of the ingot of metallurgical 316L stainless steel and its pipes. For good corrosion resistance, 316L stainless steel vascular stents with ultra-low carbon content were prepared in this work. The evaluation of in vitro toxicity and in vivo reliability was carried out.

3.2 Structure and morphology of MIM stents

Images of the MIM stents are shown in Fig. 4. As shown in the figure, the as-received stents exhibited a complete shape, and no nodes, stains, cracks, or other defects were found on the surface.

The SEM images of surfaces of the MIM vascular stents are shown in Fig. 5. The surface appears somewhat rough because the stent was produced through a powder metallurgy route, and the porosity was expected. Furthermore, many original powder particles were observed on the side surfaces of the stents, as shown in Figs. 5(e) and (f). An electrical polishing process is required to remove these residual powder particles.

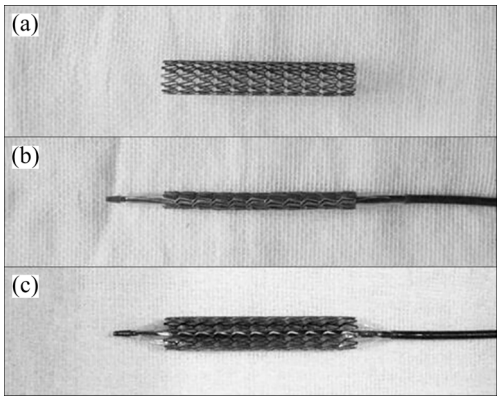

Fig. 4 MIM vascular stents in as-received (a), folded (b), and expanded (c) states

The MIM vascular stents showed a completely austenite structure with grain sizes ranging from 20 to 100 μm. Some residual pores were also observed. The composition and size of the grains on the outer layer were similar to those in the center, which indicated that MIM technology could realize a completely homogenous microstructure.

3.3 In vitro cytotoxicity

As shown in Fig. 6, the morphology of the

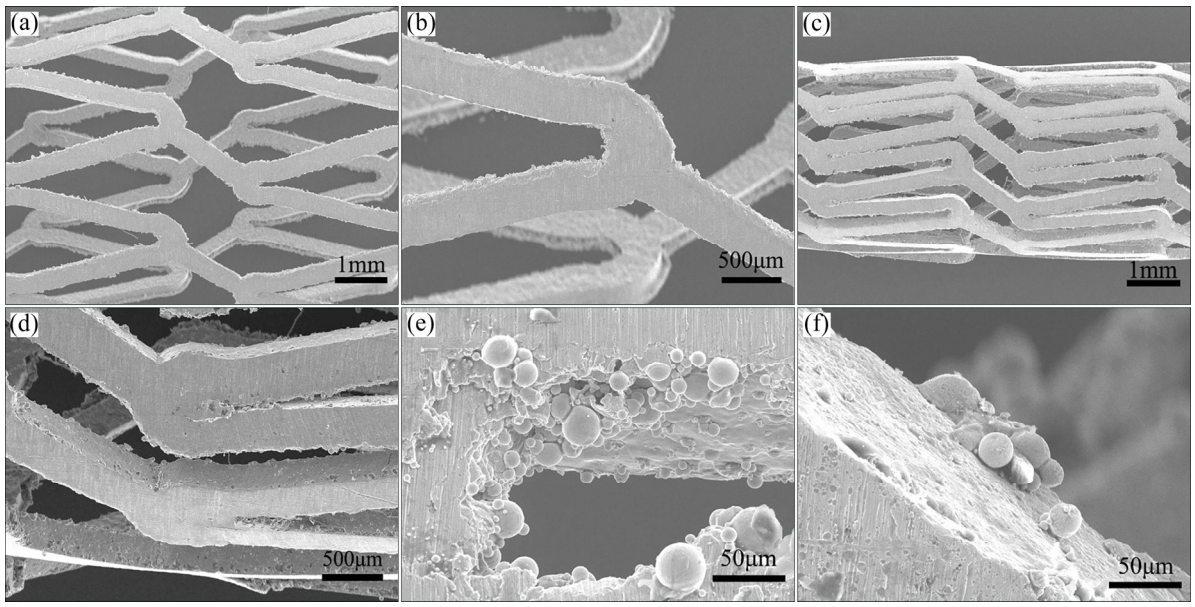

Fig. 5 SEM images of MIM vascular stents in expanded (a, b), and folded (c, d) states, and powder particles affiliated to stents (e, f)

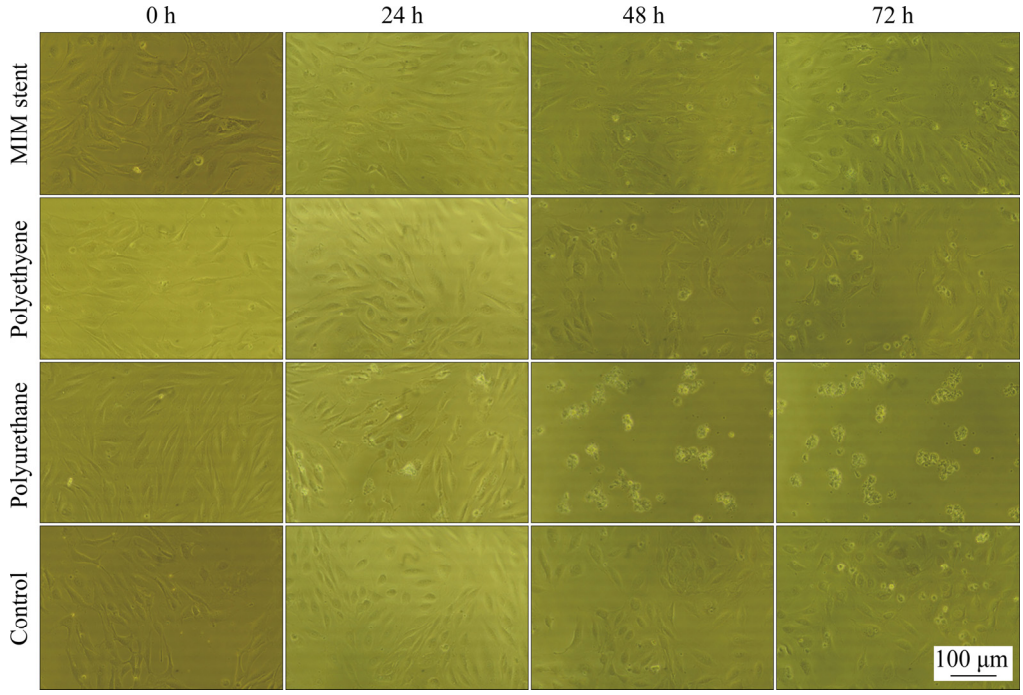

Fig. 6 Microscopic views of in vitro cytotoxicity (The morphology of the HUVECs in the stent and polyethylene indicated that the cells were normal. HUVECs in the polyurethane group started to be lysed from 24 h)

MIM stent, polyethylene, and control groups was normal, while there was massive death of HUVECs treated with liquid extracts of polyurethane at 48 and 72 h. The CCK-8 cell viability assay (Fig. 7) was consistent with the microscopic observation. The cell viabilities of the MIM stent and polyethylene groups were high, while that of polyurethane was low, which proved the efficiency of the liquid extraction process. These results demonstrated that the MIM stent had no obvious cell cytotoxicity.

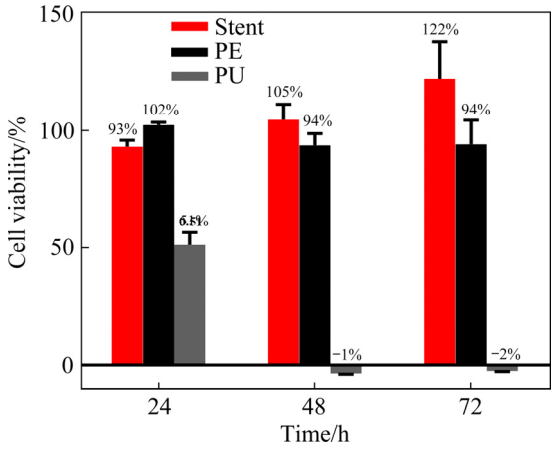

Fig. 7 Cytotoxic experiment results indicating cell viability of HUVECs treated with liquid extracts of MIM stent, polyethylene, and polyurethane at 24, 48, and 72 h (The viabilities of the stent and polyethylene groups were higher than 70%, while that of polyurethane was lower than 70%. Stent: MIM vascular stent; PE: Polyethylene; PU: Polyurethane)

3.4 In vivo biomedical behavior of MIM vascular stents

The implantation procedure was successful. All dogs safely underwent the endovascular procedure. The procedure time, anesthesia time, intraoperative fluid replacement volume, intraoperative blood loss, and other operation data were recorded. There were no statistical differences among different dogs. The dogs were fed for a maximum of a 6-month observation period after the operation. Activity, dietary, and mental status were observed and recorded. All eight dogs survived with good physiological and psychological status during the observation period. There was no evidence of vessel rupture, dissection, aneurysm or pseudoaneurysm formation, carcinoma, or other anomalies occurring in our series of animal studies during the experimental observation period.

The perioperative data are shown in Table 2. Digital subtraction angiography (DSA) was performed on the dogs at selected time; the observed dogs were randomly chosen. Figure 8 shows the DSA results of a dog with implanted stents. According to the DSA results, migration,

Table 2 Perioperative data of canine experiment

Test No.	Iliac artery (L/R)	Diameter of LIA/mm	Diameter of RIA/mm	Diameter of AA/mm	Diameter of stent*/mm	Length of stent*/cm
1	L	4.36	4.31	6.82	4.73	3.89
2	R	3.93	4.02	7.40	4.36	3.79
3	L	4.25	4.10	7.24	5.01	3.85
4	L	4.51	4.61	7.44	4.71	3.88
5	R	4.05	3.99	7.03	4.42	3.82
6	R	4.67	4.63	6.66	4.97	3.92
7	R	4.39	4.25	6.91	4.63	3.88
8	R	4.59	4.35	6.71	4.53	3.86

L: Left; R: Right; LIA: Left iliac artery; RIA: Right iliac artery; AA: Abdominal aorta. *Diameters were measured and noted after MIM stent implantation. All data were collected in the angiography laboratory

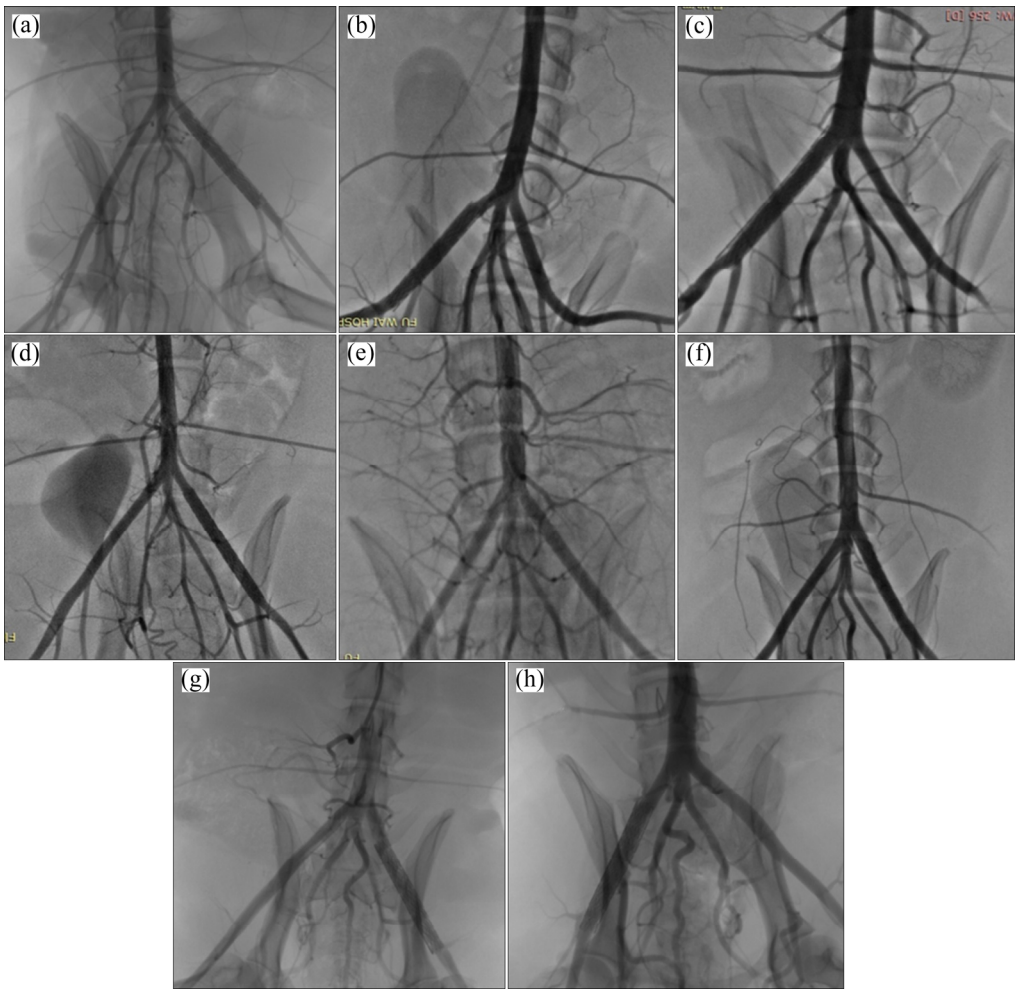

Fig. 8 DSA results: (a−d) DSA images of four dogs in 1-month group showing favorable results, indicating patency of stent without any adverse events; (e−h) DSA images of four dogs in 6-month group showing desirable results as well

twist, collapse, infection, acute or chronic thrombosis, stenosis, and obstruction of the stents were not observed during the entire observation period. These results indicate that the stents can provide considerable supporting strength from a relatively small metal surface area, and the vessel is compatible with the stent within a short time.

Bare metal stents are endothelialized within a short time. The implanted stents and iliac arteries obtained from the dogs are shown in Fig. 9. The

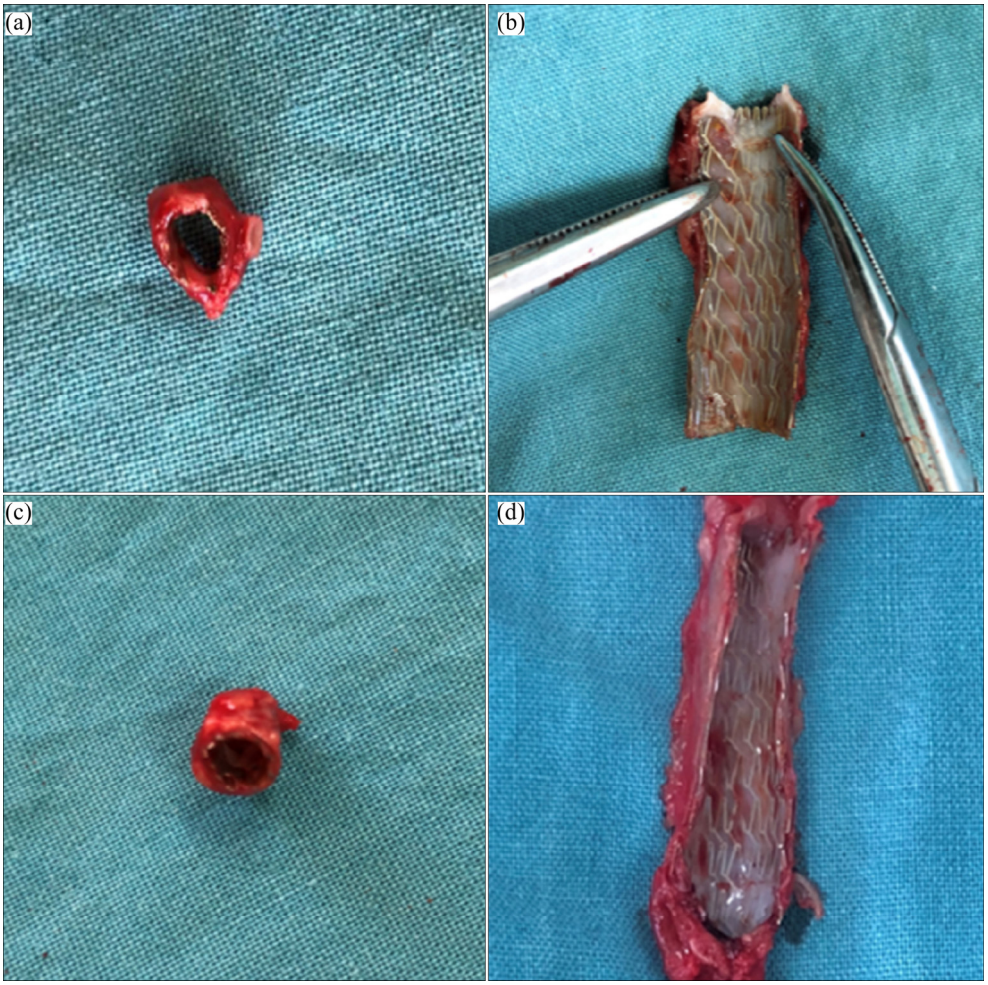

Fig. 9 Neointima formation during observation period: (a, b) Neointimal area in 1-month group; (c, d) Neointimal area in 6-month group

structure of the iliac artery adjacent to the stents was also observed using an optical microscope. The stents were in contact but were not affiliated with the inner walls of the iliac artery. Observations showed that the surface of the stent was covered by a thin layer of new endothelial cells, which was connected by the adjacent endothelium. The 6-month group had a higher new endothelium coverage rate than the 1-month group.

Based on the results of TUNEL (Fig. 10) and Verhoeff's van Gieson (EVG) staining (Fig. 11), stent implantation did not cause significant inflammatory cell infiltration, elastic plate rupture, significant apoptosis, or other adverse effects. Further observation by scanning electron microscopy confirmed the neointima of the stent. The results showed that the coverage of endothelial cells in the 6-month group increased compared with that in the 1-month group ((98.50±2.40)% versus (94.00±2.85)%, p<0.01). The expression levels of CD31, CD34, CD133, and eNOS were determined using qPCR. The results showed that the expression levels of CD31, CD34, CD133, and NOS3 in the experimental group were higher than those in the control group. The expression level of CD31 in the 6-month experimental group was higher than that in the 1-month experimental group, and the expression level of CD34 was similar in the two experimental groups. In contrast, the expression levels of eNOS in the 6-month experimental group were lower than those in the 1-month experimental group (Fig. 12).

All the experimental dogs tolerated the implantation procedure well and showed good physical and mental conditions during the observation time up to 6 months. The DSA results indicated the integrity of the stents and patency of the targeted iliac artery. All these results implied

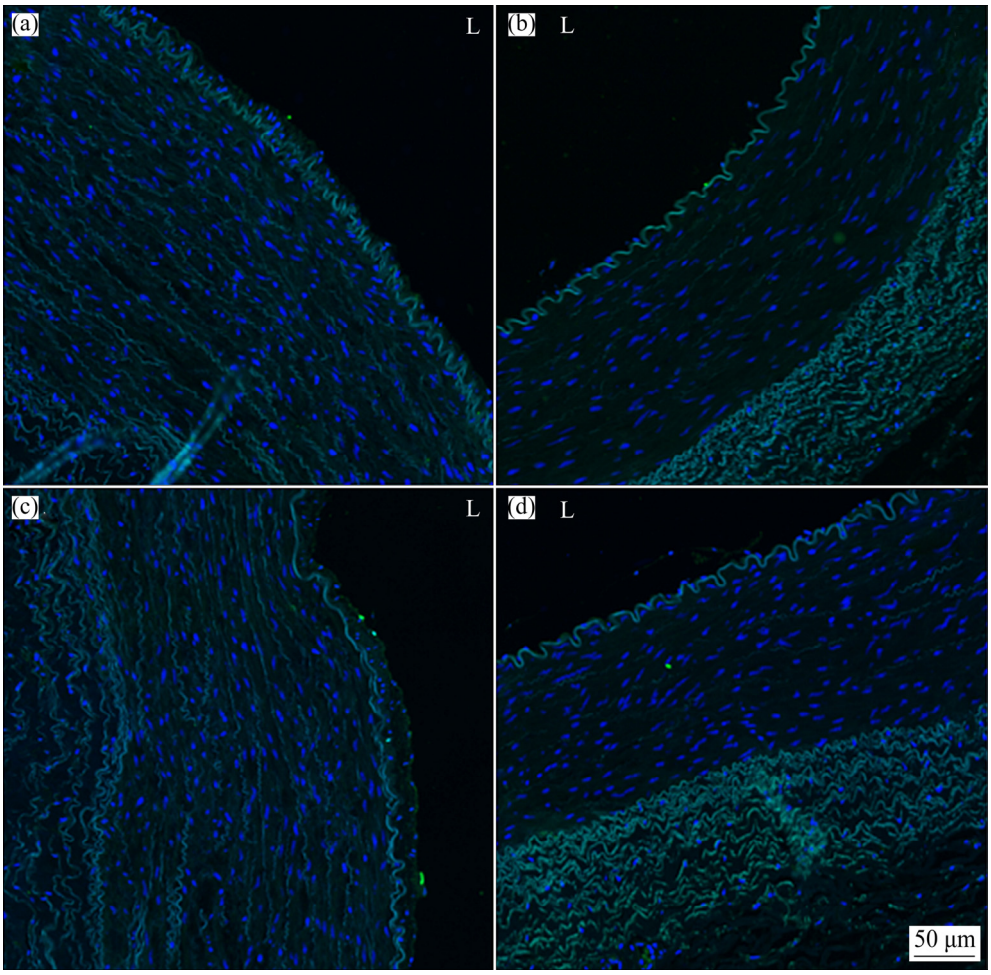

Fig. 10 Observation results of TUNEL staining on intra-luminal side: (a) Experimental group in 1-month observation group; (b) Control group in 1-month observation group; (c) Experimental group in 6-month observation group; (d) Control group in 6-month observation group (L: Intra-luminal side)

that the MIM stents had good biocompatibility, although longer observation periods were still warranted. The implanted MIM stents were endothelialized quite quickly without in-stent thrombosis, which was confirmed by observation and analyses using optical microscopy. Endothelialization plays an important role in the prevention of in-stent thrombosis, and in-stent stenosis, which contributes to the uneventful results of the present experiments, provides evidence for the biocompatibility of the MIM stents. A molecular biological analysis of the canine iliac arteries showed that the expression levels of CD31, CD34, CD133, and NOS3 in the experimental group were higher than those in the control group. As indicated by several studies, CD31, CD34, CD133, and NOS3 are immune cell markers that have several protective functions including maintaining the integrity of endotheliums, participating in endothelialization procedures, and repairing vascular damage; thus, they can be used as evaluation indexes for stents and grafts [17−20]. These results indicate excellent prognosis after stent implantation and support good biocompatibility of MIM stents, despite the limited sample size in the initial experiment.

Overall, the MIM 316L stent exhibited good performance and biocompatibility. Mainstream methods for manufacturing vascular stents include laser cutting and metal wire braiding, both of which require sophisticated techniques, expensive equipment investment, and long production periods. Moreover, these traditional methods may lead to unsatisfactory geometric properties, such as nodes and uneven microstructures, which could increase the risk of restenosis

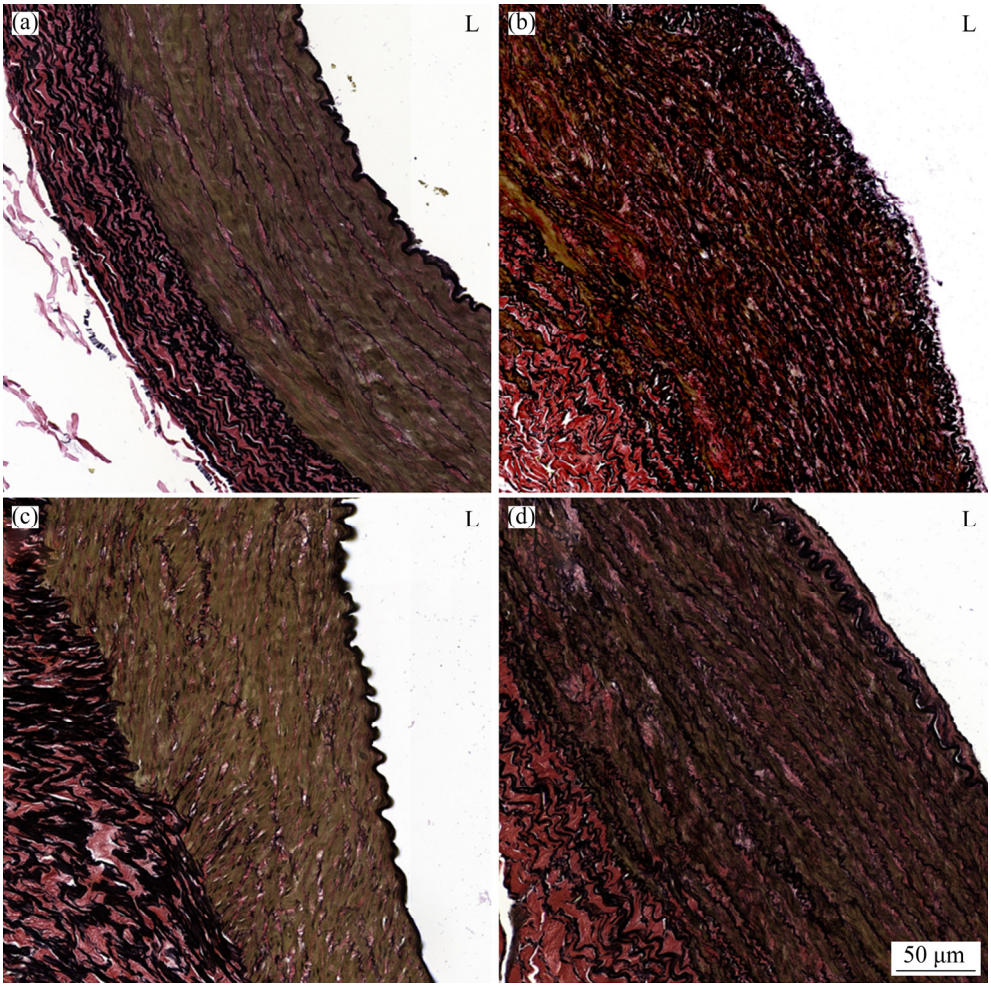

Fig. 11 Optical microscopic observation of vascular wall by Verhoeff's van Gieson (EVG): (a) Experimental group in 1-month observation group; (b) Control group in 1-month observation group; (c) Experimental group in 6-month observation group; (d) Control group in 6-month observation group (L: Intra-luminal side)

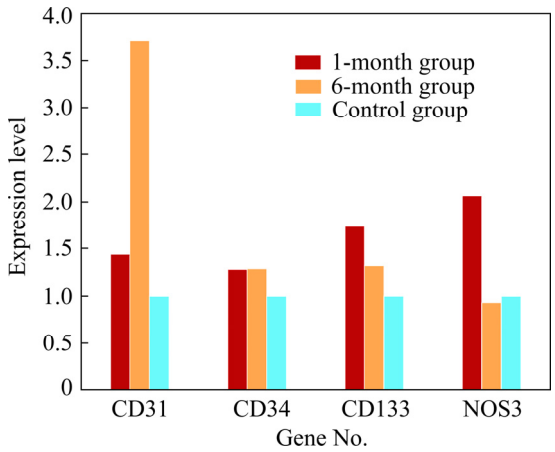

Fig. 12 Expression levels of Genes CD31, CD34, CD133, and NOS3

after stent implantation. Therefore, it is necessary to develop more economical and advanced technologies to manufacture vascular stents. Compared with laser cutting and braiding, metal injection molding technology considerably improves the utilization of stent materials and enriches its more powerful batch and customized attributes. To the best of our knowledge, this study is the first to develop vascular stents using the MIM method and validate their biocompatibility and safety in experimental animals. Further studies are required in other material systems as well to investigate mechanical fatigue reliability and biological safety.

4 Conclusions

(1) MIM 316L stainless steel specimens with different carbon contents were prepared, and the effect of carbon content fluctuation on their mechanical properties and corrosion resistance was

studied. The performance of 316L stainless steel is very sensitive to the carbon content. Carbon content fluctuation should be precisely controlled during MIM.

(2) In vitro cytotoxic experiments showed that the MIM 316L stents had no significant cytotoxicity. The stents manufactured using MIM could maintain a stable form and structure with fast endothelialization of the luminal surface of the stent; they could also ensure long-term patency in animal models. They demonstrated favorable structural, physical, and chemical stability as well as biocompatibility, indicating their promising potential for application in clinical practice.

Acknowledgments

The authors are grateful for the financial supports from the Major Project of the Ministry of Science and Technology of Changsha, China (No. kh2003014), the Hunan Provincial Natural Science Foundation, China (Nos. 2018JJ2584, 2018JJ3507), the Beijing Municipal Science and Technology Comission, China (No. D171100002917004), and the Guangxi Science and Technology Plan Project, China (No. AD16380019).

References

[1] MANI G, FELDMAN M D, PATEL D, AGRAWAL C M. Coronary stents: A materials perspective [J]. Biomaterials, 2007, 28(9): 1689−1710.

[2] WYKRZYKOWSKA J J, KRAAK R P, HOFMA S H, VAN DER SCHAAF R J, ARKENBOUT E K, IJSSELMUIDEN A J, ELIAS J, VAN DONGEN I M, TIJSSEN R Y G, KOCH K T, BAAN J, VIS M M, DE WINTER R J, PIEK J J, TIJSSEN J G P, HENRIQUES J P S, AIDA INVESTIGATORS. Bioresorbable scaffolds versus metallic stents in routine PCI [J]. The New England Journal of Medicine, 2017, 376(24): 2319−2328.

[3] BRILAKIS E S, EDSON R, BHATT D L, GOLDMAN S, HOLMES D R Jr, RAO S V, SHUNK K, RANGAN B V, MAVROMATIS K, RAMANATHAN K, BAVRY A A, GARCIA S, LATIF F, ARMSTRONG E, JNEID H, CONNER T A, WAGNER T, KARACSONYI J, KINLAY S. Drug-eluting stents versus bare-metal stents in saphenous vein grafts: A double-blind, randomised trial [J]. The Lancet, 2018, 391(10134): 1997−2007.

[4] INOUE T, CROCE K, MOROOKA T, SAKUMA M, NODE K, SIMON D I. Vascular inflammation and repair: Implications for re-endothelialization, restenosis, and stent thrombosis [J]. JACC: Cardiovascular Interventions, 2011, 4(10) 1057−1066.

[5] LOU J, LI Y M, HE H, LI D Y, WANG G Y, FENG J, LIU C. Interface development and numerical simulation of powder co-injection moulding. Part I: Experimental results on the flow behaviour and die filling process [J]. Powder Technology, 2017, 305: 405−410.

[6] HE H, LOU J, LI Y M, ZHANG H, YUAN S, ZHANG Y, WEI X S. Effects of oxygen contents on sintering mechanism and sintering-neck growth behaviour of FeCr powder [J]. Powder Technology, 2018, 329: 12−18.

[7] LI J G, CHEN L, ZHANG X Q, GUAN S K. Enhancing biocompatibility and corrosion resistance of biodegradable Mg−Zn−Y−Nd alloy by preparing PDA/HA coating for potential application of cardiovascular biomaterials [J]. Mater Sci Eng C: Mater Biol Appl, 2020, 109: 110607.

[8] DING Y, ZHAO A S, LIU T, WANG Y N, GAO Y, LI J A, YANG P. An injectable nanocomposite hydrogel for potential application of vascularization and tissue repair [J]. Annals of Biomedical Engineering, 2020, 48(5): 1511−1523.

[9] GUERRA A J, CIURANA J. 3D-printed bioabsordable polycaprolactone stent: The effect of process parameters on its physical features [J]. Materials & Design, 2018, 137: 430−437.

[10] PARK J, KIM J K, KIM D S, SHANMUGASUNDARAM A, PARK S A, KANG S, KIM S H, JEONG M H, LEE D W. Wireless pressure sensor integrated with a 3D printed polymer stent for smart health monitoring [J]. Sensors and Actuators B: Chemical, 2019, 280: 201−209.

[11] PARK S A, LEE S J, LIM K S, BAE I H, LEE J H, KIM W D, JEONG M H, PARK J K. In vivo evaluation and characterization of a bio-absorbable drug-coated stent fabricated using a 3D-printing system [J]. Materials Letters, 2015, 141: 355−358.

[12] DEHGHAN-MANSHADI A, YU P, DARGUSCH M, STJOHN D, QIAN M. Metal injection moulding of surgical tools, biomaterials and medical devices: A review [J]. Powder Technology, 2020, 364: 189−204.

[13] ZHAO D P, CHEN Y K, CHANG K K, EBEL T, LUTHRIGNER-FEYERABEND B J C, WILLUMEIT-RÖMER R, PYCZAK F. Surface topography and cytocompatibility of metal injection molded Ti−22Nb alloy as biomaterial [J]. Transactions of Nonferrous Metals Society of China, 2018, 28: 1342−1350.

[14] CARLSON J M. Metal injection molded tubing for drug eluting stents: United States patent, US8303642B1 [P]. 2012−11−06.

[15] MARIOT P, LEEFLANG M A, SCHAEFFER L, ZHOU J. An investigation on the properties of injection-molded pure iron potentially for biodegradable stent application [J]. Powder Technology, 2016, 294: 226−235.

[16] DUBÉ H, CLIFFORD A G, BARRY C M, SCHWARTEN D E, SCHWARTZ L. Comparison of the vascular responses to balloon-expandable stenting in the coronary and peripheral circulations: Long-term results in an animal model using the TriMaxx stent [J]. Journal of Vascular Surgery, 2007, 45: 821−827.

[17] RAFII S, LYDEN D. Therapeutic stem and progenitor cell transplantation for organ vascularization and regeneration [J]. Nature Medicine, 2003, 9: 702−712.

[18] URBICH C, DIMMELER S. Endothelial progenitor cells: Characterization and role in vascular biology [J]. Circulation Research, 2004, 95: 343−353.

[19] WIISANEN M E, ABDEL L-LATIF A, MUKHERJEE D, ZIADA K M. Drug-eluting stents versus bare-metal stents in saphenous vein graft interventions: a systematic review and meta-analysis [J]. JACC: Cardiovascular Interventions, 2010, 3: 1262−1273.

[20] ZHANG B, ZHENG B, WANG X G, SHI Q P, JIA J, HUO Y, PAN C S, HAN J Y, CHEN M. Polymer-free dual drug-eluting stents evaluated in a porcine model [J]. BMC Cardiovascular Disorders, 2017, 17: 1−11.

金属粉末注射成型制备血管支架的实验动物生物相容性

舒 畅[1,2]，何 昊[1]，范博文[2]，李杰华[1]，王 暾[1]，李东阳[3]，李益民[3,4]，何 浩[4]

1. 中南大学 湘雅二医院 血管外科，长沙 410011；
2. 中国医学科学院 阜外医院 血管外科，北京 100037；
3. 中南大学 粉末冶金国家重点实验室，长沙 410083；
4. 广西科技大学 微电子与材料工程学院，柳州 545006

摘 要：通过临床动物实验评价金属注射成型(MIM)制备的新型血管支架的可行性与安全性。采用粉末注射成型技术制备血管支架，大幅提高材料利用率；研究 MIM 过程中碳杂质含量变化对 316L 不锈钢力学性能与耐腐蚀性能的影响；同时开展 MIM 血管支架的体外毒性测试与动物实验以评价支架的安全性。结果表明，316L 不锈钢的性能对碳含量变化极为敏感，在 MIM 制备过程中应该对碳含量波动实施精准控制。所有 MIM 血管支架都成功植入狗的主动脉血管， MIM 316L 不锈钢支架未出现明显毒性，能够稳定维持支架形状及结构，快速实现内皮化过程，呈长期植入通畅性。采用 MIM 技术制备的新型血管支架具备合适的结构、物理以及化学稳定性和生物相容性，在临床实践中具有广阔应用前景。

关键词：血管支架；金属注射成型；细胞毒性试验；动物实验；生物相容性

(Edited by Wei-ping CHEN)